J. Earth Planet. Sci. Nagoya Univ., Vol. 50, 1 to 12, 2003

Chemical Th-U-total Pb isochron ages of zircon and monazite from granitic rocks of the Negele area, southern Ethiopia

Tadesse Yihunie

Geological Survey of Ethiopia, P.O. Box 2302, Addis Abeba, Ethiopia
(Received September 10, 2003 / Accepted December 25, 2003)

ABSTRACT

CHIME (Chemical Th-U-total Pb Isochron Method) age determinations were made on zircon and monazite grains from granitoid samples in the Negele area of southern Ethiopia. A 611±32 Ma zircon age was obtained from a syn-tectonic hornblende-biotite granite of the Alghe domain. A 453±29 Ma zircon age and a 459±16 Ma monazite age were also obtained from post-tectonic two-mica granites of the Alghe domain and the Kenticha domain, respectively. Since these ca. 450 Ma zircon and monazite ages coincide well, a significant post-tectonic granitic magmatism appears to have occurred in southern Ethiopia in early Paleozoic time.

The new CHIME age results indicate at least two episodes of granitic magmatism in southern Ethiopia in the late Proterozoic to early Paleozoic, with a ca. 150 Ma interval between syn- and post-tectonic granitic emplacements, and have an important geochronological constraint on the evolution of the East African Orogen.

INTRODUCTION

Negele (5°20'N, 39°30'E) is located in southern Ethiopia, some 200km to the north from the Kenyan border. Neoproterozoic rocks in the Negele area (Fig. 1) comprise high-grade gneissic rock associations and low-grade volcano-sedimentary and mafic-ultramafic sequences of the East African Orogen (Stern, 1994). The low-grade sequences are exposed in the Adola, Bulbul, and Moyale areas and are in structural contact with the gneissic rocks. The gneissic rocks include biotite-hornblende and biotite gneisses together with mylonitic gneisses of granitic composition and granitic migmatite, whereas variable proportions of amphibole schist/amphibolite, metabasalt, ultramafic schists, serpentinite, semi-pelitic and graphitic schists constitute the low-grade sequences (Training for Mineral Exploration Project, 1991; Gichile, 1991; Genzebu et al., 1994; Gobena et al., 1997; Yihunie and Tesfaye, 1998).

Syn-tectonic hornblende-biotite to biotite granites and post-tectonic biotite to two-mica granites intruded into the Alghe high-grade gneissic rocks, whereas late- to post-tectonic biotite to two-mica granites intruded into the low-grade rocks (Fig. 2). The granitic rocks have calc-alkaline chemical character and most of them show I-type granitic characteristics. These rocks exhibit peraluminous nature on the alumina saturation index of White and Chappel (1983). However, some of them are not typical I-type granite with high silica, total alkali, Nb and Zr contents and are generally mica (muscovite)-bearing granitoid (Yihunie, 2002).

According to previous geochemical, geochronological and isotopic studies (e.g. Rogers et al., 1965; Gilboy, 1970; Ayalew and Gichile, 1990; Abraham et al., 1992; Gichile and Fyson, 1993; Teklay et al., 1993; Worku, 1996; Wolde et al., 1996; Hussien, 1999; Yibas, 2000; Yibas et al., 2000), the Pan-African deformation, metamorphism, and magmatism in the Neoproterozoic of southern Ethiopia appear to have lasted from 880 to 500 Ma. Ggeochronological data for these rocks, however, are still not enough to sufficiently constrain the Pan-African tectono-magmatic events and the Neoproterozoic crustal growth in southern Ethiopia.

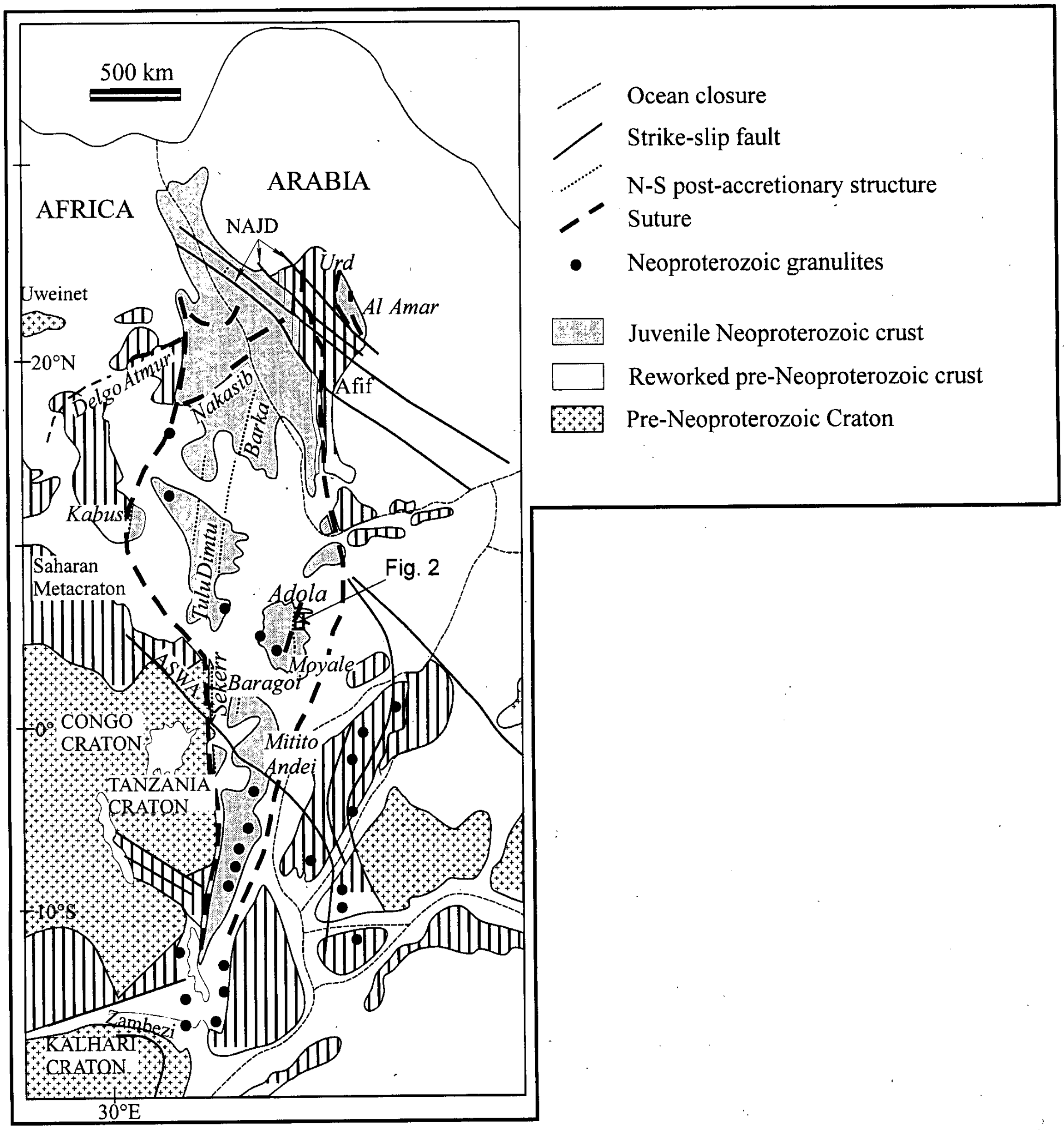

Fig. 1 Reconstructed configuration of the East African Orogen in Africa and surrounding regions showing the location of the Negele area (boxed) (modified from Abdelsalam and Stern, 1996, Hussien, 1999 and Stern, 2002).

We here report new CHIME ages of zircon and monazite from syn- and post-tectonic granites of the Negele area in southern Ethiopia and discuss their meaning.

REGIONAL GEOLOGY AND PETROGRAPHY OF GRANITIC ROCKS

High-grade gneissic rock associations and low-grade volcano-sedimentary and mafic-ultramafic sequences, which form structurally bounded north-south trending lithotectonic domains, constitute the Neoproterozoic of southern Ethiopia (Kazmin, 1972; Tefera et al., 1996; Gobena et al., 1997; Genzebu et al., 1994; Yihunie and Tesfaye,

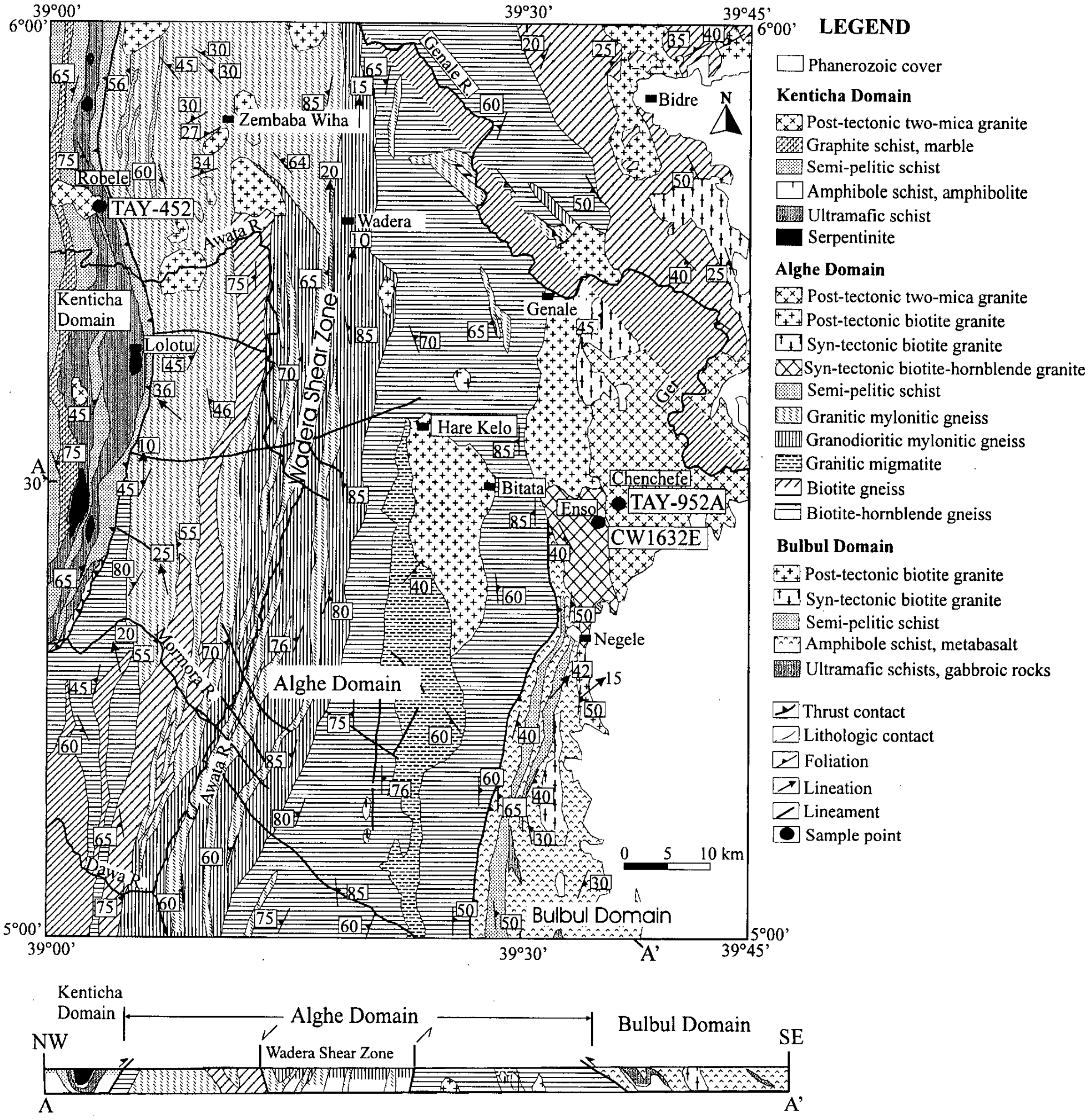

Fig. 2 Geological map showing the lithotectonic domains, major rock associations and granitic rocks of the Negele area (modified from Yihunie and Tesfaye, 1998).

1998). These metamorphic rocks were intruded by granitoid and gabbroic bodies. The high-grade gneisses are intruded dominantly by granitoids together with rare gabbroic bodies, whereas low-grade sequences are intruded dominantly by gabbro with minor granites (Training for Mineral Exploration Project, 1991; Genzebu et al., 1994; Gobena et al., 1997; Yihunie and Tesfaye, 1998).

Granitic rocks of the Negele area are dominantly biotite granite, with minor amounts of hornblende-biotite and two-mica granites. Field mapping, textural and structural evidence show that syn-tectonic hornblende-biotite and biotite granite, and post-tectonic biotite and two-mica granites occur in the Alghe gneissic domain. Granitic rocks in the Kenticha domain are commonly post-tectonic two-mica granites, whereas those in the Bulbul domain are syn- and post-tectonic biotite granites. Field and petrographic descriptions of these rocks are outlined below.

Granitic rocks from the Alghe domain

Syn-tectonic hornblende-biotite granite

There are two types of syn-tectonic granites in the Alghe domain: hornblende-biotite granite and biotite granite. Hornblende-biotite granite extends from south of the Negele town to the Enso locality to the north (see Fig. 2). It is medium- to coarse-grained foliated rock, with preferred orientation of biotite, hornblende and felsic minerals. It is often porphyritic and characterized by asymmetric quartz and feldspar phenocrysts, suggesting that it has experienced weak deformation and metamorphism. Hornblende-biotite granite is composed mainly of quartz, microcline, plagioclase, biotite, hornblende, sphene and ilmenite, with accessories of apatite, zircon, allanite and tourmaline. Epidote, chlorite, sericite and carbonate occur as secondary minerals.

Biotite granite commonly forms isolated north-south trending ridges in the northern and northeastern parts of the Alghe domain (see Fig. 2). Deformed biotite granite bodies occur as pods and lenses within granitic migmatite, biotite and biotite-hornblende gneisses. These bodies often show variations in texture and mica mineral abundance.

Post-tectonic biotite granite

Biotite granite is heterogeneous and porphyritic in texture. In places, gneissic rocks occur as enclaves and large xenoliths within this granitic body (Yihunie and Tesfaye, 1998). Some biotite granites form mountains and chain of ridge masses. Intrusive contacts with adjacent gneissic rocks were not observed. Intensely jointed and weathered granitie at the Bitata village (see Fig. 2) contains large garnet grains. In the northern part, the granite is cut by 1-2 m wide pegmatite dikes.

Biotite granite is composed mainly of biotite, quartz, plagioclase, microcline and opaque minerals. Accessory minerals include short to long prismatic euhedral to subhedral zircon, monazite, allanite, sphene, apatite, muscovite and epidote group minerals. Carbonate, chlorite and sericite occur as secondary minerals in some samples.

Post-tectonic porphyritic two-mica granite

Microcline-megacrystic muscovite-biotite granite occurs extensively in the area cut deeply by the Genale River (see Fig. 2). It is porphyritic and contains large muscovite flakes in places. During field survey, boulder-size floats of amphibole schist were locally noted, but no enclaves or xenoliths were found in two-mica granite. Locally pegmatitic dikes cut this granite. The granite is composed mainly of quartz, microcline, plagioclase, biotite and sphene. Accessory minerals include muscovite/ sericite, zircon, apatite, monazite, opaque minerals and dark brown iron-oxides.

Granitic rocks from the Kenticha domain

Post-tectonic two-mica granite

Post-tectonic two-mica granites, which intruded into the Kenticha volcano-sedimentary sequence, form large hill masses and vary from typical two-mica granite to muscovite granite/pegmatite. They are mainly massive but porphyritic in texture. Two-mica granite is composed largely of microcline, plagioclase, quartz and biotite, with trace amounts of muscovite, epidote, apatite, opaque minerals, reddish brown Fe-oxides, chlorite, zircon and monazite. In some samples biotite shows preferred orientation that may represent primary planar structure formed during magmatic emplacement.

Granitic rocks from the Bulbul domain

Syntectonic biotite granite

Syn-tectonic biotite granite in the vicinity of the Bulbul thrust is marginally sheared and occurs as unmappable small bodies intruding amphibole schist. It forms an isolated ridge mass in the southern part, where it is covered by Jurassic limestone (Yihunie and Tesfaye, 1998). Although variations in texture, mica mineral abundance and intensity of alterations are locally prominent, it is medium-grained and foliated with biotite flakes. The biotite granitie, which crops out close to the western margin of the Bulbul volcano-sedimentary sequence, is sheared; quartz ribbons, marginal recrystallization of quartz and feldspar phenocrysts are characteristic.

Biotite granite is composed mainly of quartz, microcline, plagioclase and biotite, with accessories of sphene, zircon, chlorite, sericite, epidote group and opaque minerals. Zircon is often short prismatic euhedral to subhedral.

Post-tectonic biotite granite

Post-tectonic biotite granite, which forms small hill masses and unmappable bodies, locally intruded into the Bulbul volcano-sedimentary sequence. Biotite granite is commonly altered, medium-grained, porphyritic and heterogeneous, and is composed mainly of quartz, microcline, plagioclase, biotite, with trace amounts of sphene, zircon, opaque minerals and reddish brown iron oxides. Secondary minerals include chlorite, sericite and epidote group minerals. Some biotite granite exhibits a texture similar to the rapakivi texture, where biotite flakes form cluster.

CHIME DATING RESULTS

Zircon and monazite grains were analyzed on a JEOL JCXA-733 electron microprobe analyzer. The analytical procedures and CHIME age calculations are as described in Suzuki and Adachi (1991; 1994). The ThO_2, UO_2 and PbO contents of the analyzed spots of zircon and monazite grains and corresponding apparent ages are listed in Tables 1–3. The PbO vs. UO_2^* or ThO_2^* diagrams are shown in Figs. 3–5.

Table 1. ThO_2, UO_2 and PbO contents of zircons for the analyzed spots and corresponding apparent ages (Ma) from syn-tectonic hornblende-biotite granite of the Alghe domain.

Sample No. CW1632E

Spot No.	ThO_2	UO_2	PbO	Age	UO_2^*
Z01-01	0.077	0.149	0.015	619	0.172
Z01-02	0.033	0.083	0.008	590	0.093
Z01-03	0.016	0.032	0.004	737	0.036
Z01-04	0.056	0.227	0.022	642	0.243
Z02-01	0.082	0.164	0.016	616	0.189
Z02-02	0.039	0.054	0.006	615	0.066
Z02-03	0.175	0.139	0.018	668	0.191
Z02-04	0.026	0.074	0.007	615	0.084
Z02-05	0.023	0.077	0.007	577	0.084
Z02-06	0.077	0.063	0.008	616	0.086
Z02-07	0.135	0.102	0.013	645	0.143
Z02-08	0.241	0.136	0.019	640	0.208
Z02-09	0.117	0.105	0.013	639	0.140
Z02-10	0.094	0.140	0.014	603	0.169
Z02-11	0.028	0.052	0.005	568	0.060
Z03-01	0.087	0.136	0.015	638	0.162
Z03-02	0.048	0.085	0.009	671	0.099
Z03-03	0.057	0.109	0.011	605	0.126
Z03-04	0.037	0.086	0.008	578	0.097
Z04-01	0.037	0.068	0.008	702	0.079
Z04-02	0.073	0.192	0.020	656	0.213
Z04-03	0.077	0.115	0.012	635	0.138
Z05-01	0.502	0.854	0.016	116	1.011
Z05-02	0.060	0.576	0.037	454	0.594
Z05-03	0.150	0.702	0.032	315	0.748
Z05-04	0.564	0.137	0.013	316	0.310
Z05-05	0.251	0.122	0.018	630	0.197
Z05-06	0.036	0.055	0.006	598	0.065
Z05-07	0.228	0.106	0.014	557	0.174
Z06-01	0.091	0.094	0.009	555	0.121
Z06-02	0.330	0.138	0.019	574	0.237
Z06-03	0.072	0.065	0.008	637	0.087

Table 2. ThO_2, UO_2 and PbO contents of zircons for the analyzed spots and corresponding apparent ages (Ma) from post-tectonic two-mica granite of the Alghe domain.

Sample No. TAY952A

Spot No.	ThO_2	UO_2	PbO	Age	UO_2^*
Z01-01	0.039	0.141	0.010	482	0.152
Z01-02	0.075	0.098	0.008	490	0.120

Z01-03	0.039	0.253	0.015	408	0.264
Z01-04	1.019	0.681	0.035	256	0.995
Z01-05	0.559	0.396	0.032	407	0.566
Z01-06	0.228	0.225	0.019	453	0.295
Z01-07	0.099	0.123	0.009	443	0.153
Z02-01	0.043	0.033	0.004	543	0.046
Z02-02	0.033	0.052	0.004	467	0.062
Z02-03	0.014	0.015	—	—	—
Z02-04	0.050	0.048	0.005	607	0.063
Z03-01	0.068	0.068	0.007	534	0.088
Z03-02	0.011	0.258	0.006	176	0.261
Z04-01	0.021	0.043	0.004	512	0.049
Z04-02	0.013	0.020	—	—	—
Z04-03	0.023	0.073	0.005	440	0.080
Z04-04	0.069	0.367	0.026	477	0.387
Z04-05	0.050	0.070	0.006	508	0.085
Z05-01	0.058	0.314	0.021	454	0.332
Z05-02	0.155	0.762	0.027	249	0.810
Z05-03	0.103	0.530	0.016	209	0.562

Table 3. ThO_2, UO_2 and PbO contents of monazites for the analyzed spots and corresponding apparent ages (Ma) from post-tectonic two-mica granite of the Kenticha domain.

Sample No. TAY452

Grain No.	**ThO_2**	**UO_2**	**PbO**	**Age**	**UO_2***
M01	10.5	0.397	0.230	458	11.8
M02-01	11.2	0.630	0.254	449	13.3
M02-02	12.3	0.663	0.274	446	14.5
M02-03	8.33	0.550	0.192	445	10.1
M02-04	9.19	0.602	0.221	466	11.2
M02-15	10.2	0.623	0.242	466	12.2
M02-06	14.5	0.720	0.323	452	16.8
M02-07	14.3	0.706	0.327	462	16.7
M02-08	10.5	0.625	0.246	459	12.6
M03-01	10.7	0.604	0.253	468	12.7
M03-02	8.62	0.520	0.202	460	10.3
M03-03	10.7	0.628	0.248	456	12.8
M03-04	12.6	0.641	0.293	470	14.7
M03-05	11.7	0.600	0.265	455	13.7
M03-06	11.3	0.645	0.268	469	13.4
M03-07	10.7	0.667	0.259	471	12.9
M04-01	9.70	0.247	0.208	465	10.5
M04-02	10.2	0.265	0.211	448	11.1
M04-03	9.20	0.229	0.194	458	9.96
M04-04	7.88	0.170	0.158	442	8.44
M04-05	7.89	0.193	0.172	474	8.52
M04-06	7.57	0.167	0.158	458	8.12
M04-07	7.40	0.143	0.152	456	7.87
M04-08	6.71	0.152	0.144	468	7.21
M04-09	6.65	0.126	0.138	458	7.06

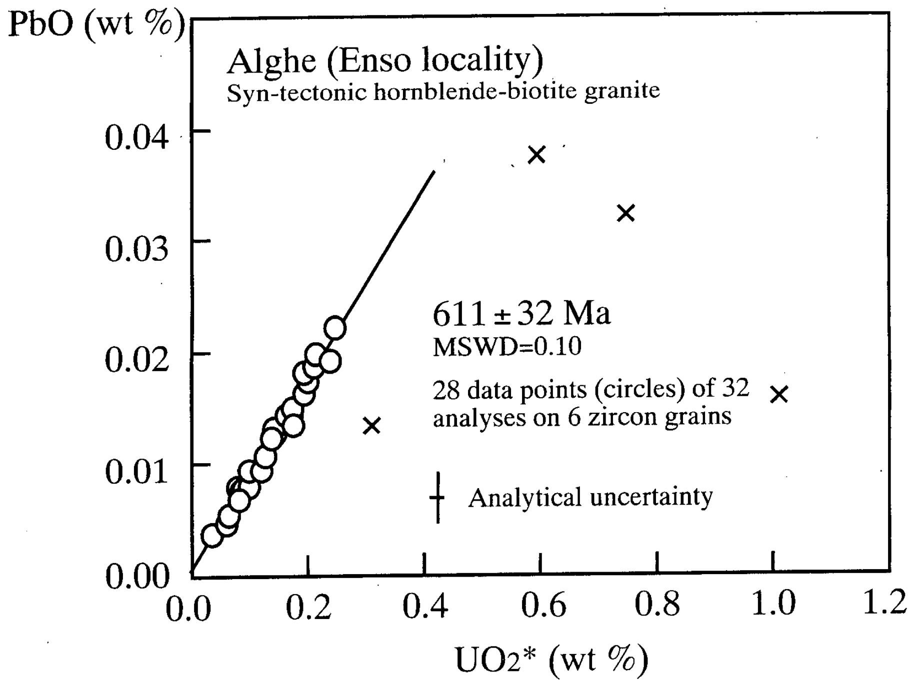

Fig. 3 PbO vs. UO_2^* (corrected UO_2: UO_2 plus the equivalent of ThO_2) plots of zircons in syn-tectonic hornblende-biotite granite from Enso locality of the Alghe domain. Circles represent data points for clear portions and crosses represent metamict portions. Error bars in the figure represent 2σ analytical uncertainty. Data from Table 1.

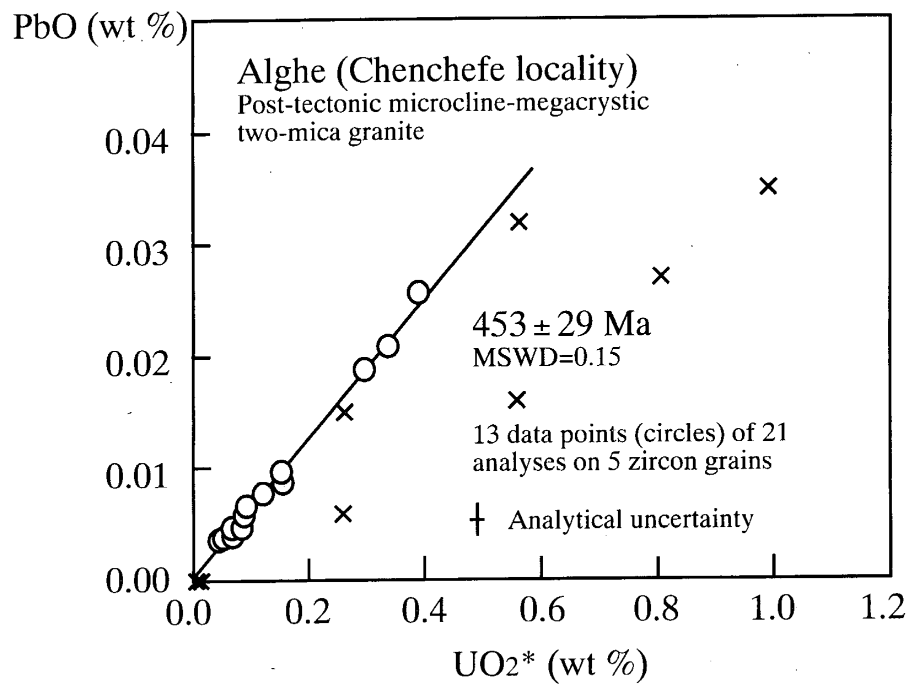

Fig. 4 PbO vs. UO_2^* (corrected UO_2: UO_2 plus the equivalent of ThO_2) plots of zircons in post-tectonic microcline-megacrystic two-mica granite from Chenchefe locality of the Alghe domain. Circles represent data points for clear portions and crosses represent metamict portions. Error bars in the figure represent 2σ analytical uncertainty. Data from Table 2.

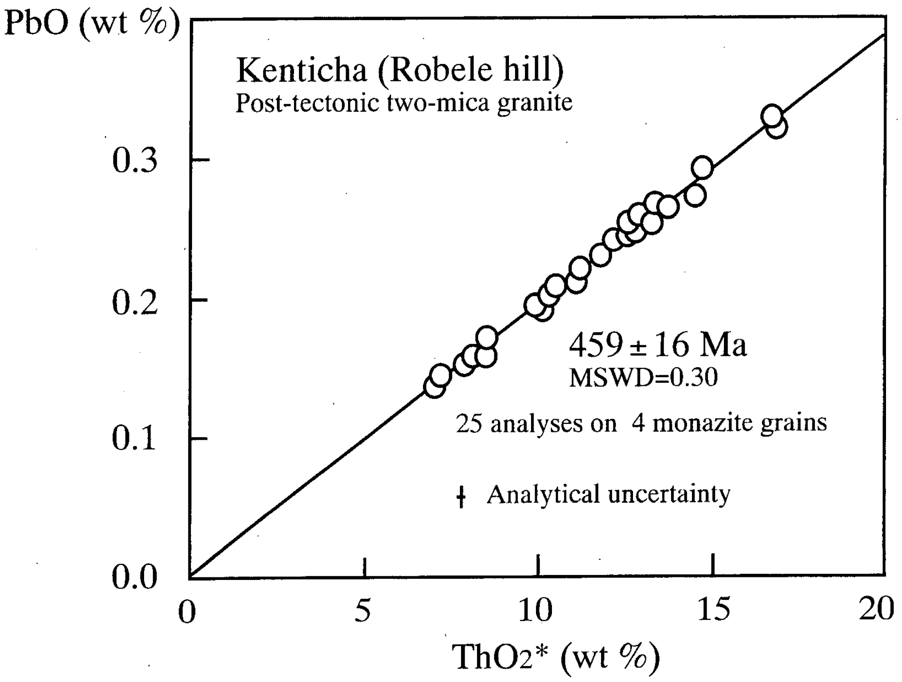

Fig. 5 PbO vs. ThO_2* (corrected ThO_2: ThO_2 plus the equivalent of UO_2) plots of monazites in posttectonic two-mica granite from Robele hill of the Kenticha domain. Error bars in the figure represent 2σ analytical uncertainty. Data from Table 3.

Syn-tectonic hornblende-biotite granite (CW1632E in Fig. 2)

A total of 32 spots on six inclusion-free euhedral to subhedral zircon from hornblende-biotite granite of the Alghe domain were analyzed and the analytical data are given in Table 1. Except for four metamict spots, 28 data points were plotted on the PbO vs. UO_2* diagram (Fig. 3). In the analyzed zircon grains, the ThO_2 concentration ranges from 0.016 to 0.564%, while UO_2 and PbO contents vary from 0.032 to 0.854% and 0.0048 to 0.0374%, respectively. On the PbO vs. UO_2* diagram, the data points on clear portions (circles) are well aligned and give an isochron age of 611±32 Ma (MSWD=0.10) with an intercept of 0.0002±0.0005. Since the regression line passes through the origin of the PbO vs. UO_2* diagram, secondary Pb-loss is considered to be insignificant. The 611±32 Ma zircon age can be interpreted as the emplacement age for the hornblende-biotite granite.

Post-tectonic two-mica granite (TAY952A in Fig. 2)

A total of 21 spots on five zircon grains from microcline-megacrystic two-mica granite of the Alghe gneissic domain were analyzed. The analytical data are presented in Table 2. The ThO_2, UO_2 and PbO contents in the analyzed zircon grain vary from 0.011 to 1.02%, 0.033 to 0.762% and 0.0040 to 0.0346%, respectively. Two spots (Z02-03 and Z04-02) contain PbO below the detection limit (0.0035). Analytical data are plotted on the PbO vs. UO_2* diagram (Fig. 4). Thirteen data points on clear portions (circles) show linear arrangement on the PbO vs. UO_2* diagram and the regression line yields an isochron age of 453±29 Ma (MSWD=0.15) with an intercept of 0.0005±0.0004. The CHIME age is interpreted as a crystallization age for the two-mica granite.

Post-tectonic two-mica granite (TAY452 in Fig. 2)

Twenty-five spots on four monazite grains from two-mica granite of the Kenticha domain were analyzed and the analytical data are given in Table 3. The data are plotted on the PbO vs. ThO_2* diagram (Fig. 5). In the analyzed monazite grains, the ThO_2, UO_2 and PbO contents vary from 6.65 to 14.5%, 0.126 to 0.720% and 0.138 to 0.327%, respectively. On the PbO vs. ThO_2* diagram, a well-defined linear array of data points gives an isochron age of 459±16 Ma (MSWD=0.30) with an intercept of 0.0005±0.0079. This age is interpreted to show the time of post-tectonic granite intrusion into the Kenticha metavolcano-sedimentary and mafic-ultramafic sequence during the late Pan-African orogeny.

DISCUSSION AND CONCLUSIONS

The newly obtained CHIME zircon and monazite ages have the geochronological constraints on the emplacement or crystallization ages of granitic plutons in southern Ethiopia. The CHIME age (611±32 Ma) of zircons from syn-tectonic hornblende-biotite granite is correlatable to that of the syn-tectonic Gariboro granitic massif (zircon U-Pb 646±30 Ma; Worku, 1996) in the Adola belt. The CHIME zircon and monazite ages (453±29 Ma and 459±16 Ma) from the post-tectonic granitic rocks are younger than the age reported for similar post-tectonic plutonic rocks in this region; the upper limit age for the Pan-African orogeny in southern Ethiopia has been ca. 500 Ma. However, since the 453±29 Ma CHIME zircon age coincides well with the 459±16 Ma monazite age, the ca. 450 Ma age is considered to represent some important chronological event. Evidently our CHIME age data show a ca. 150 Ma interval between the syn- and post-tectonic granitic plutons. This time gap as well as the mineralogical, structural and textural variations in the granitic rocks (Yihunie, 2002) suggest episodic granitic magmatism in southern Ethiopia.

Similar episodic granitic magmatism was also recognized for the Pan-African orogenic processes in the Neoproterozoic of western Ethiopia (Ayalew et al., 1990; Kebede et al., 2001; Kebede and Koeberl, 2003) and northern Ethiopia (Alemu, 1997; Tadesse et al., 2000). The emplacement or crystallization ages of granitic rocks and their role for crustal growth of the Arabian-Nubian Shield during the Pan-African orogeny have been discussed by several workers (e.g. Jackson et al., 1984; Jackson, 1986; Lenoir et al., 1994).

Geochemical features of granitic rocks in the East African Orogen are considerably variable with regard to the emplacement time and tectonic environments of their formation. Most granitic rocks apear to exhibit calc-alkaline chemical character and are dominantly of I-type along with some A-type granites, suggestive of their formation at subduction-related to collisional and/or post-collisional tectonic environments (White and Chappel, 1983; Pearce et al., 1984; Whalen et al., 1987). Geochemical data of granitic rocks (Yihunie, 2002) may support this inference. Whalen et al. (1987) suggested that A-type chemical character of the granitic rocks, may not necessarily indicate anorogenic nature, because they occur in different tectonic environments of formation through geologic time. One of the authors (T.Y.) favors the possibility of granitic magmatism in a subduction-related to collisional and/or post-collisional tectonic environments during the Pan-African orogeny in the Neoproterozoic. This point will be discussed in a separate paper in a little more detail.

In summary, the new CHIME age data obtained from the granitic rocks of the Negele area clearly show at least two episodes of granitic emplacement in southern Ethiopia. This suggests that the evolution of Pan-African crust and associated tectono-magmatic events have lasted longer than previously thought (Stern, 1994).

ACKNOWLEDGEMENTS

We thank S. Yogo for his help during thin section preparation and S. Tanaka for his assistance during carbon coating of the thin sections analyzed by EPMA. Constructive comments and suggestions by Prof. M. Hoshino significantly improved the contents of the manuscript. Finally, T. Y. thanks the Ministry of Education, Science and Culture, Japan for the financial support.

REFERENCES

Abdelsalam, M.G. and Stern, R.J. (1996) Sutures and shear zones in the Arabian-Nubian Shield. Jour. African Earth Sci. 23, 289–310.

Abraham, A., Nassir, H., Yemane, T., Genzebu, W., Seyid, G., Mehari, K. and Alemu, T. (1992) Geological evolution of the Proterozoic of southern Ethiopia. 29th International Geological Congress, Abstracts 2, Kyoto, 272.

Alemu, T. (1997) Petrology, geochemistry and geochronology of granitoids from the Axum area. M.Sc. thesis, University of Vienna, Austria, 106p.

Ayalew, T. and Gichile, S. (1990) Preliminary U-Pb ages from southern Ethiopia. 15th Colloquium of African Geology, Nancy, Extended abstracts, 127–130.

Ayalew, T., Bell, K., Moore, J.M. and Parrish, R.R. (1990) U-Pb and Rb-Sr geochronology of the Western Ethiopian Shield. Geol. Soc. Amer. Bull. 102, 1309–1316.

Genzebu, W., Hassen, N. and Yemane, T. (1994) Geology of the Agere Maryam area (NB37-10). Ethiopian Institute of Geological Surveys, Addis Abeba. (Memoir 8), 112p.

Gichile, S. (1991) Structure, metamorphism and tectonic setting of a gneissic terrane, the Segen-Afelata area, southern Ethiopia. M.Sc. Thesis, University of Ottawa, Canada, 225p.

Gichile, S. and Fyson, W.K. (1993) An inference of the tectonic setting of the Adola belt of southern Ethiopia from the geochemistry of magmatic rocks. Jour. African Earth Sci. 16, 235–246.

Gilboy, C.F. (1970) The geology of the Gariboro region of southern Ethiopia. Ph.D. Thesis, University of Leeds. United Kingdom, 1–176.

Gobena, H., Belayneh, M., Kebede, T., Tesfaye, S. and Abraham, A. (1997) Geology of the Dodola area (NB37-7). Ethiopian Institute of Geological Surveys, Addis Abeba. (Memoir 10), 144p.

Hussien, B. (1999) The geology, structure and geochemistry of the crystalline rocks of the Moyale area, southern Ethiopia: implications for the tectonogenesis of the Precambrian basement. Ph.D. Thesis, Tubinger Geowissenschaftliche Arbeiten (TGA), Band 50, 102p.

Jackson, N.J. (1986) Petrogenesis and evolution of Arabian felsic plutonic rocks. Jour. African Earth Sci. 4, 47–59.

Jackson, N.J., Walsh, J.N. and Pegrem, E. (1984) Geology, geochemistry and petrogenesis of the late Precambrian granitoids in the central Hijaz region of the Arabian Shield. Contrib. Mineral. Petrol. 87, 205–219.

Kazmin, V. (1972) In: The Geology of Ethiopia Note No. 821-051-12. Ethiopian Institute of Geological Surveys, Addis Abeba, 208p.

Kebede, T., Kloetzli, U.S., Koeberl, C. (2001) U/Pb and Pb/Pb zircon ages from granitoid rocks of Wallagga area: constraints on magmatic and tectonic evolution of Precambrian rocks of western Ethiopia. Mineral. Petrol. 71, 251–271.

Kebede, T., Koeberl, C. (2003) Petrogenesis of A-type granitoids from the Wallagga area, western Ethiopia: constraints from mineralogy, bulk-rock chemistry, Nd and Sr isotopic compositions. Precamb. Res. 121, 1–24.

Lenoir J.-L, Küster, D., Liegeois, J.-P., Utke, A., Haider, A., Matheis, G. (1994) Origin and regional significance of late Precambr. Rund. 83, 624–641.

Pearce, J.A., Harris, N.B.W. and Tindle, G.A. (1984) Trace element discrimination diagrams for the tectonic interpretation of granitic rocks. Jour. Petrol. 25, 956–983.

Rogers, A.S., Miller, J.M. and Mohr, P.A. (1965) Age determinations on some Ethiopian basement rocks. Nature 206, 1021–1023.

Stern, R.J. (1994) Arc assembly and continental collision in the Neoproterozoic East African Orogen: implications for the consolidation of Gondwanaland. Ann. Rev. Earth Planet. Sci. 22, 319–351.

Stern, R.J. (2002) Crustal evolution in the East African Orogen: a neodymium perspective. Jour. African Earth Sci. 34, 2002.

Suzuki, K. and Adachi, M. (1991) Precambrian provenance and Silurian metamorphism of the Tsubonosawa paragneiss in the south Kitakami terrane, northeast Japan, revealed by the chemical Th-U-total Pb isochron ages of monazite, zircon and xenotime. Geochem. Jour. 25, 357–376.

Suzuki, K. and Adachi, M. (1994) Middle Precambrian detrital monazite and zircon from the Hida gneiss on Oki-Dogo island, Japan: their origin and implication for the correlation of basement gneiss of southwest Japan and Korea. Tectonophysics 235, 277–292.

Tadesse, T., Hoshino, M., Suzuki, K. and Iizumi, S. (2000) Sm-Nd, Rb-Sr and Th-U-Pb zircon ages of syn- and post-tectonic granitoids from the Axum area of northern Ethiopia. Jour. African Earth Sci. 30, 313–327.

Tefera, M., Chernet, T. and Haro, W. (1996) Explanation to the Geological map of Ethiopia, 2nd ed. (1:2,000,000). Ethiopian Institute of Geological Surveys, Addis Abeba, 79p.

Teklay, M., Kröner, A. and Oberhansli, R. (1993) Reconnaissance Pb-Pb zircon ages from Precambrian rocks in eastern and southern Ethiopia and an attempt to define crustal provinces. In: Thorweihe, U. and Schandelmeier, H. (eds.) Geoscientific Research in Northeast Africa, Balkema, Rotterdam, 133–138.

Training for Mineral Exploration Project (1991) The geology of Adola area (1:100,000). Ethiopian Institute of Geological Surveys, Addis Abeba.

Whalen, J.B., Currie, K.L. and Chappel, B.W. (1987) A-type granites: geochemical characteristics, discrimination and petrogenesis. Contrib. Mineral. Petrol. 95, 407–419.

White, A.J.R. and Chappel, B.W. (1983) Granitoid types and their distribution in the Lachlan Fold Belt, southeastern Australia. Geol. Soc. Am., Memoir 159, 21–34.

Wolde, B., Asres, Z., Desta, Z. and Gonzalez, J.J. (1996) Neoproterozoic zirconium depleted boninite and tholeiitic series rocks from Adola, southern Ethiopia. Precamb. Res. 80, 261–279.

Worku, H. (1996) Geodynamic development of the Adola belt (southern Ethiopia) in the Neoproterozoic and its control on gold mineralization. Ph.D. Thesis, Technical University of Berlin, Wissenschaftliche Schriftenreihe Geologie und Bergbau, Band5, Berlin.

Yibas, B. (2000) The Precambrian geology, tectonic evolution and controls of gold mineralization in southern Ethiopia. Ph.D. dissertation, University of Witwatersrand, Johannesburg, 448p.

Yibas, B., Reimold, W.U. and Anhausser, C.R. (2000) The geological evolution of the Precambrian of southern Ethiopia. The 27th Earth Science Congress of the Geological Society of South Africa, Stellenbosch, South Africa, Abstracts 16–17.

Yihunie, T. (2002) Structure, petrology and geochemistry of Neoproterozoic rocks from the Negele area, southern Ethiopia. Ph.D. Thesis, Nagoya University, 105p.

Yihunie, T. and Tesfaye, M. (1998) Geology of the Negele area (NB37-11). Ethiopian Institute of Geological Surveys, Addis Abeba, (Memoir 11), 124p.